



Contents lists available at ScienceDirect

## Fusion Engineering and Design

journal homepage: [www.elsevier.com/locate/fusengdes](http://www.elsevier.com/locate/fusengdes)

## Model-based control of the resistive wall mode in DIII-D: A comparison study

J. Dalessio<sup>a</sup>, E. Schuster<sup>a,\*</sup>, D.A. Humphreys<sup>b</sup>, M.L. Walker<sup>b</sup>, Y. In<sup>c</sup>, J.-S. Kim<sup>c</sup><sup>a</sup> Department of Mechanical Engineering and Mechanics, Lehigh University, 19 Memorial Drive West, Bethlehem, PA 18015, USA<sup>b</sup> General Atomics, 3550 General Atomics Court, San Diego, CA 92121, USA<sup>c</sup> Far-Tech Inc., 3550 General Atomics Court, Building 15, Suite 155, San Diego, California 92121, USA

## ARTICLE INFO

## Article history:

Available online 10 March 2009

## Keywords:

Fusion plasma physics  
Resistive wall modes  
Model-based control  
Robust stabilization

## ABSTRACT

One of the major non-axisymmetric instabilities under study in the DIII-D tokamak is the resistive wall mode (RWM), a form of plasma kink instability whose growth rate is moderated by the influence of a resistive wall. One of the approaches for RWM stabilization, referred to as magnetic control, uses feedback control to produce magnetic fields opposing the moving field that accompanies the growth of the mode. These fields are generated by coils arranged around the tokamak. One problem with RWM control methods used in present experiments is that they predominantly use simple non-model-based proportional-derivative (PD) controllers requiring substantial derivative gain for stabilization, which implies a large response to noise and perturbations, leading to a requirement for high peak voltages and coil currents, usually leading to actuation saturation and instability. Motivated by this limitation, current efforts in DIII-D include the development of model-based RWM controllers. The General Atomics (GA)/Far-Tech DIII-D RWM model represents the plasma surface as a toroidal current sheet and characterizes the wall using an eigenmode approach. Optimal and robust controllers have been designed exploiting the availability of the RWM dynamic model. The controllers are tested through simulations, and results are compared to present non-model-based PD controllers. This comparison also makes use of the  $\mu$  structured singular value as a measure of robust stability and performance of the closed-loop system.

© 2009 Elsevier B.V. All rights reserved.

## 1. Introduction

The resistive wall mode (RWM) is a form of plasma kink instability that deforms the entire plasma configuration symmetrically in the helical direction with an extremely fast MHD Alfvénic time scale ( $\sim \mu\text{s}$ ). The presence of the conductive tokamak structure acts as a stabilizing mechanism through the eddy currents that are induced by the time-varying magnetic perturbations generated by the plasma deformation. These induced currents generate magnetic fields that oppose the plasma deformation, resulting in a slower growth time ( $\sim \text{ms}$ ) of the RWM, which allows the use of feedback to control this mode [1]. The inherent resistive losses of the surrounding structure cause a decay in the induced wall currents reducing the stabilizing effect of the wall. Current research focuses on the stabilization of the first ( $n = 1$ ) kink mode (the plasma perturbation repeats only once as the toroidal angle varies from 0 to  $2\pi$ ) since this is usually the first to occur when pressure increases.

There have been many successful efforts on feedback stabilization of resistive wall modes in DIII-D [2] as well as in other tokamaks such as HBT-EP [3], NSTX [4], and ITER, and in reversed field pinch devices such as EXTRAP T2R [5] and RFX-mod [6]. Most of the sta-

bilizing efforts in this field focused on designing non-model-based, empirically-tuned controllers with PD (proportional-derivative) action, without taking advantage of developed models. One problem with PD controllers used in present experiments is that they require substantial derivative gain for stabilization, which implies a large response to noise and perturbations, leading to a requirement for high peak voltages and coil currents. Model-based controllers have the potential of overcoming this limitation by exploiting the a-priori knowledge (model) of the system. There have been already some efforts in this direction [7,8], which have been proved effective through simulation in increasing to some extent the stability region of the closed-loop system.

The GA/Far-Tech DIII-D RWM model replaces the perturbed plasma surface by a perturbed toroidal current sheet, and models the resistive wall using an eigenmode approach [9,10]. The plasma surface and current sheet perturbations are equivalent in the sense that they both produce the same magnetic field perturbation. Using Faraday's Law, a set of inductive circuit equations form the state space model that embeds a scalar coupling coefficient  $c_{pp}$ , which is inversely related to the growth rate  $\gamma$  of the mode. Although the plasma surface deformation cannot be directly measured in real time, the magnitude and phase of the deformation can be diagnosed from measurements by a set of 22 magnetic field sensors composed of poloidal magnetic field probes and saddle loops, which measure radial flux. Using an estimator for the two orthogonal components

\* Corresponding author. Tel.: +1 610 758 5253.

E-mail address: [schuster@lehigh.edu](mailto:schuster@lehigh.edu) (E. Schuster).

of the assumed  $n = 1$  mode pattern, the 22 outputs are reduced to 2 outputs that represent the sine and cosine components of the RWM. These two outputs can be combined to express the output as a signal composed of the RWM amplitude and toroidal phase [11]. The quartet configuration for the internal feedback control coils (I-coils) reduces the number of controllable inputs by locking the phase of the I-coils in sets of four,  $120^\circ$  apart. Thus, the original 12 I-coils used to return the plasma to its original axisymmetric shape are reduced to 3 circuits (system inputs).

The overall goal of this work is to use the developed DIII-D RWM model to design optimal and robust model-based feedback controllers for RWM stabilization over a predefined range of the growth rate  $\gamma$ , extending the stability range of present non-model-based PD controllers. By designing controllers that can robustly stabilize the RWM and meet specified controller performance criteria over a large range of growth rates we eliminate the need of online identification and controller scheduling when the growth rate varies during the discharge.

## 2. Plasma model

The matrices in the model represent characteristics of the tokamak and are well known. The uncertainty is introduced through the variable  $c_{pp}$ , which corresponds to a certain growth rate  $\gamma$  of the resistive wall mode. The relationship between these variables is further explained in [10].

The model is represented in terms of the couplings between the plasma (p), vessel wall (w), and coils (c). The model derived from Faraday's law of induction results in the system dynamics that reduce to

$$(M_{ss} - M_{sp}c_{pp}M_{ps})\dot{I}_s + R_{ss}I_s = V_s \quad (1)$$

where  $M_{ss}$  is the mutual inductance between external conductors, including the vessel wall and the coils,  $M_{sp}$  is the mutual inductance between external conductors and the plasma (and  $M_{ps} = M_{sp}^T$ ),  $R_{ss}$  is the resistance matrix,  $I_s$  is the current flowing in the conductors, and  $V_s$  is the externally applied voltage to the conductors. The current and externally applied voltage to the conductors can be written as  $I_s = [I_w^T \ I_c^T]^T$  and  $V_s = [0^T \ V_c^T]^T$ , where  $I_w$  is the wall current,  $I_c$  is the coil current, and  $V_c$  is the externally applied voltage to the coil.

This model can be represented in a state space formulation using the current in the conductors as the states ( $x = I_s$ ) and the applied voltage as the inputs ( $u = V_s$ ). This results in the state equation

$$\dot{x} = Ax + Bu + w_1 \quad (2)$$

where  $A = -L_{ss}^{-1}R_{ss}$ , and  $B = L_{ss}^{-1}$ , with  $L_{ss} = M_{ss} - M_{sp}c_{pp}M_{ps}$ . The output equation is given by

$$y = Cx + w_2 \quad (3)$$

with  $C = \tilde{C}\bar{C}$ , where  $\tilde{C}$  denotes the mode estimator and  $\bar{C} = C_{ss} - C_{yp}c_{pp}M_{ps}$ .  $C_{yp}$  denotes the coupling matrix between the magnetic sensors and the plasma current, and  $C_{ss} = [C_{yw} \ C_{yc}]$  is given by the coupling matrices between the sensors and the wall ( $C_{yw}$ ) and coil ( $C_{yc}$ ) currents. The state space system model includes the noise effect, where  $w_1$  is the process noise and  $w_2$  is the measurement noise, which are assumed to be zero-mean with covariances  $Q = E(w_1 w_1^T)$  and  $R = E(w_2 w_2^T)$ , where  $E$  denotes the expectation operator.

## 3. Model-based advanced control design

### 3.1. Optimal control (time domain)

Besides achieving closed-loop stability, we are interested in designing a control law  $u = Ky$  that minimizes the mode ampli-

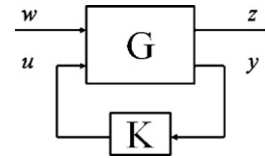


Fig. 1. Plant model.

tude  $y$  and the control power  $u$  (contributing to actuator saturation avoidance), i.e.,

$$\min_K J = \frac{1}{2} \int_0^\infty (y^T Q_y y + u^T R_u u) dt \quad (4)$$

where  $Q_y$  and  $R_u$  are semi-positive and positive definite matrices defined by the designer. This a well known problem in the field of controls, and its solution is provided by Optimal Control Theory [12].

### 3.2. Robust control (frequency domain)

By using the Laplace transform [13], we obtain a frequency-domain representation of (2) and (3) given by

$$\begin{bmatrix} z \\ y \end{bmatrix} = G(s) \begin{bmatrix} w \\ u \end{bmatrix} = \begin{bmatrix} G_{11}(s) & G_{12}(s) \\ G_{21}(s) & G_{22}(s) \end{bmatrix} \begin{bmatrix} w \\ u \end{bmatrix} \quad (5)$$

$$u = K(s)y \quad (6)$$

Noise signals  $w_1$  and  $w_2$  are grouped into  $w = [w_1^T \ w_2^T]^T$ . As shown in Fig. 1, the output  $y$  is used by the controller  $K(s)$  to calculate the input  $u$ . The performance output  $z$  represents a weighted function of the control power  $u$  and the mode amplitude  $y$  that we want to minimize. We are interested in synthesizing a stabilizing controller  $K$  such that the  $\mathcal{H}_\infty$  norm (maximum energy amplification) of the transfer function  $T_{zw}(G, K)$  between input  $w$  and output  $z$  is minimized (the mode amplitude  $y$  and control power  $u$  are minimized for any input  $w$ ), i.e.,

$$\min_{K(s)} \|T_{zw}(G, K)\|_\infty = \min_{K(s)} \left( \sup_{\omega} \bar{\sigma}(T_{zw}(G, K)(j\omega)) \right) \quad (7)$$

where  $\bar{\sigma}$  denotes the maximum singular value and  $\omega$  the frequency. The combination of the Small Gain Theorem with  $\mathcal{H}_\infty$  control allows the design of controllers that are able to achieve closed-loop stability and satisfy performance requirements even when the true system and the nominal model used for design are different, i.e., the controller is robust against unmodeled dynamics. This a very well known problem in the field of control systems, and its solution is provided by Robust Control Theory [14].

## 4. Robust stability and performance

It is possible to extract the uncertain parameter  $c_{pp}$  from the uncertain state space system (2) and (3) and represent it as an uncertainty block that perturbs a nominal state space system. The majority of the complexity is introduced in the  $A$  and  $B$  state matrices, where the uncertainty  $c_{pp}$  is introduced through  $L_{ss}^{-1}$ . Since the instability is two-dimensional (sine and cosine components of the unstable mode), the matrix product  $M_{sp}M_{ps}$  is rank 2. Thus, the  $L_{ss}$  matrix can be expressed as

$$L_{ss} = M_{ss} - M_{sp}c_{pp}M_{ps} = M_{ss} - c_{pp} \sum_{i=1}^2 u_i u_i^T \quad (8)$$

where  $M_{sp} = M_{ps}^T = [u_1 \ u_2]$ , and  $u_1$  and  $u_2$  are  $n \times 1$  vectors where  $n$  is the number of states in the RWM state space model. To obtain a parameterized expression for the  $L_{ss}^{-1}$  term, we must first compute

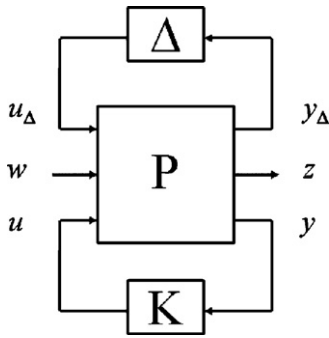


Fig. 2. General framework for robust control.

the inverse of a matrix sum. Given the matrix  $A_T$ , the scalar  $b_T$ , and the vectors  $C_T$  and  $D_T$ , the inverse of a matrix sum is given by the Sherman–Morrison formula as [15]

$$(A_T - b_T C_T D_T)^{-1} = A_T^{-1} + \frac{b_T (A_T^{-1} C_T) (D_T A_T^{-1})}{1 - b_T D_T A_T^{-1} C_T}. \quad (9)$$

Using (9) twice it is possible to express each state matrix as a general affine state space representation

$$A = \sum_{i=0}^4 \alpha_i A_i, B = \sum_{i=0}^4 \alpha_i B_i, C = C_0 + \alpha_5 C_5, \quad (10)$$

where  $\alpha_i$ 's are nonlinear functions of  $c_{pp}$ , and  $A_i$ 's,  $B_i$ 's and  $C_i$ 's are constant matrices.

By writing  $c_{pp} = c_{pp}^* + \delta e$  with

$$e = \max\{|c_{pp_{max}} - c_{pp}^*|, |c_{pp_{min}} - c_{pp}^*|\},$$

where  $c_{pp}^*$  is the nominal value of  $c_{pp}$  used to compute the matrices  $A_i$ 's,  $B_i$ 's and  $C_i$ 's, and  $c_{pp_{min}}$  and  $c_{pp_{max}}$  are its minimum and maximum values, respectively, we define a new normalized uncertainty  $\delta$  that has a range of values within  $|\delta| \leq 1$  that corresponds to the desired  $c_{pp}$  range.

The parameterization of the RWM model (see [16] for details) allows this system to be represented in the general framework of robust control for uncertain systems as shown in Fig. 2, where  $P$  represents the nominal plant and  $\Delta = \delta I$  the uncertainty of the system. Given a feedback controller  $K$ , the closed system can be computed as

$$T_{zw}(s) = F_l(F_u(P, \Delta), K) = F_u(F_l(P, K), \Delta)$$

where  $F_l$  and  $F_u$  denote the lower and upper linear fractional transformations (LFT's).

The goal is to design a controller that can robustly stabilize the RWM and meet specified controller performance criteria (minimization of the  $\mathcal{H}_\infty$  norm (maximum energy amplification) of the transfer function  $T_{zw}(G, K)$ ). The robust stability of the plant is determined by the  $N_{11}$  sub-matrix, where  $N = F_l(P, K)$  represents the nominal closed-loop system. The sub-system  $N_{11}$  term isolates the uncertainty from the input  $w$  and output  $z$  of the system, and connects  $y_\Delta$  with  $u_\Delta$ . The robust stability is determined by the structured singular value, which is defined as

$$\mu(N_{11}) \triangleq \frac{1}{\min\{k_m | \det(I - k_m N_{11} \Delta) = 0\}}$$

for  $\bar{\sigma}(\Delta) \leq 1$ . Larger  $\mu$  values means  $(I - N_{11} \Delta)$  becomes singular with small perturbations, thus the smaller  $\mu$  the better. The robust stability condition is found by finding the smallest value of  $k_m$  at the onset of instability, or  $\det(I - k_m N_{11} \Delta) = 0$ , which yields  $k_m = 1/\mu(N_{11})$ , where  $k_m$  is a measure of the robust stability to perturbations in  $\Delta$ . Thus, assuming  $N_{11}$  and  $\Delta$  are stable, the system

is robustly stable if and only if  $\mu(N_{11}(j\omega)) < 1, \forall \omega$ . Similarly, the robust performance is given by  $\mu(N(j\omega)) < 1, \forall \omega$ . Both conditions assume that  $N$  is internally stable.

## 5. Controller synthesis and simulation

### 5.1. Model-based controller design

The complete system that is used to design the controller has two additional time-delay blocks preceding the plasma model. The time delays represent the plasma control system and the power supply. For design purposes, the time delays are linearized using second order Padé approximations.

Both the optimal (LQG) and the robust (Normalized Coprime Factorization (NCF)) controllers were designed using a  $c_{pp}$  value of 0.3325 ( $\gamma = 5000$ ) using the 29 eigenmode model with 64 states. The LQG and NCF controllers were reduced after design to 8 and 12 states, respectively using the Hankel norm model reduction technique [14]. For the optimal controller, we have chosen  $Q_y = 1.0 \times 10^{-2}$  and  $R_u = 1$  weighting matrices. The noise covariance matrices are assumed  $Q = 1.0 \times 10^4$  and  $R = 3.5 \times 10^3$ .

### 5.2. Controller simulation and results

In order to be able to compare the proposed model-based controllers with present non-model-based controllers, a proportional-derivative (PD) controller is designed (integral action is not required for this system). The PD controller is synthesized to maximize the stability range as a function of  $\gamma$  and is of the form

$$K_{ij} = \frac{G_{p_{ij}} + G_{D_{ij}} s}{1 + \tau_{pcs} s} \quad (11)$$

where  $i$  is the index for the control inputs into the system ( $i = 1 \dots 3$ ),  $j$  is the index for the system outputs ( $j = 1 \dots 2$ ),  $G_{p_{ij}}$  is the proportional gain,  $G_{D_{ij}}$  is the derivative gain, and  $\tau_{pcs}$  is the time constant taken to be  $4 \times 10^{-4}$  s. Each  $K_{ij}$  term fills the  $3 \times 2$  controller matrix  $K$ . It was found that the stability range can be maximized by a controller with non-zero  $K_{11}$ ,  $K_{22}$ , and  $K_{32}$  terms and every other term set to zero. Using PD controllers for the terms  $K_{11}$ ,  $K_{22}$ , and  $K_{32}$ , all six gains are optimized to obtain the maximum range of stability as a function of  $\gamma$ . The resulting gains are  $G_{p_{11}} = 3.80 \times 10^4$ ,  $G_{D_{11}} = 76$ ,  $G_{p_{22}} = 1.38 \times 10^4$ ,  $G_{D_{22}} = 40$ ,  $G_{p_{32}} = 6.62 \times 10^4$  and  $G_{D_{32}} = 103$ .

The performance of the LQG and NCF controllers are simulated using a Simulink model of the plasma, controller, plasma control system, and power supply, and compared to the results of a well-tuned PD controller. The power supply has a saturation block that realizes the physical limit of the applied voltage of  $\pm 100$  V. Table 1 provides the performance constraints in response to a unit step in the RWM mode amplitude.

Fig. 3 shows the time response to initial conditions of the plasma, normalized to a starting RWM mode amplitude of 1 Gauss. The simulation is carried out at constant RWM growth rates of  $\gamma = 10$  rad/s and  $\gamma = 5000$  rad/s, the lower and upper limits of the growth rate range of our interest. Both model-based controllers provide quick suppression of the RWM mode amplitude, out-performing the PD

Table 1  
Performance targets and constraints.

| Condition     | Target value | Maximum constraint |
|---------------|--------------|--------------------|
| Rise time     | 1.0 ms       | 5.0 ms             |
| Settling time | 5.0 ms       | 10 ms              |
| Input voltage | N/A          | $\pm 100$ V        |

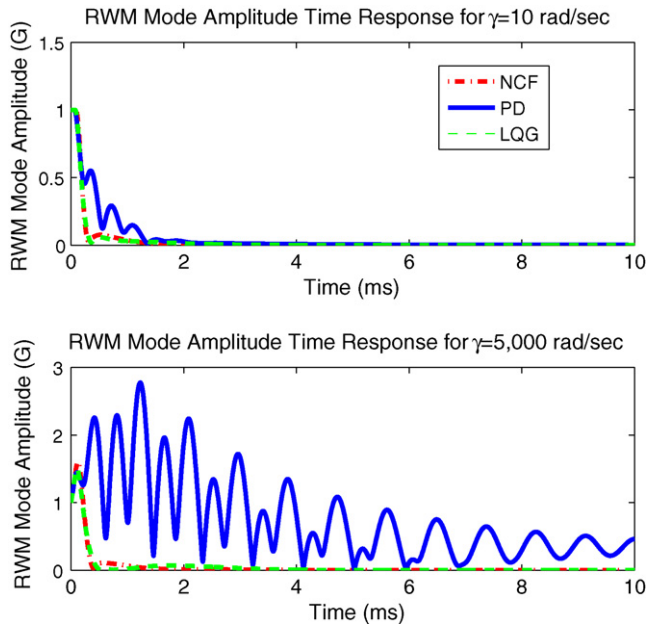


Fig. 3. Initial condition response RWM mode amplitude for  $\gamma = 10$  rad/s (top) and  $\gamma = 5000$  rad/s (bottom).

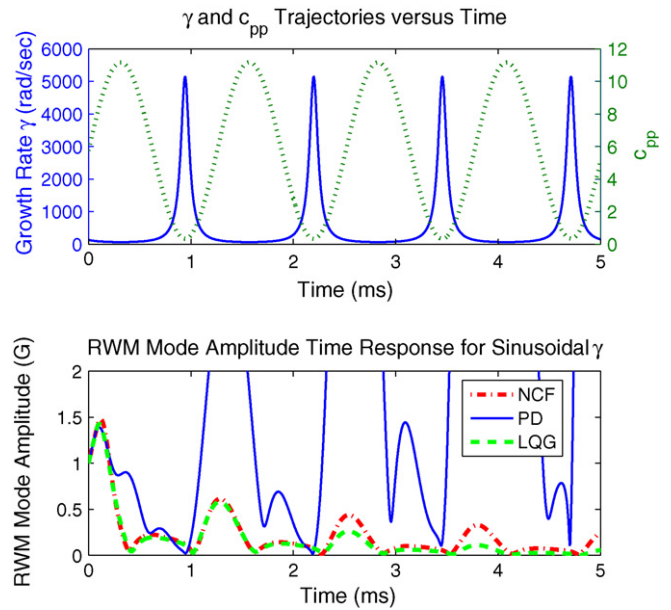


Fig. 4. Initial condition response RWM mode amplitude for sinusoidal  $c_{pp}$ .

controller, which does not provide quick suppression at the faster growth rate. In addition, the PD controller requires a much higher control power for stabilization.

5.3. Closed-loop stability and performance

It is useful to determine the range of  $\gamma$  where the system remains stable as well as the range where the system performs within the limits of the performance constraints (see Table 1). Table 2 provides the ranges of  $\gamma$  for which stability and performance conditions are satisfied. The first row (*Stability Range*) indicates the range of  $\gamma$  for which the system remains stable when using a unit step input for the RWM model amplitude. The second row (*Perf. Range (Step)*) represents the range of  $\gamma$  for which the performance conditions are satisfied under the same control input. Both model-based controllers show good stability and performance properties well beyond the desired  $\gamma$  range and that of the PD controller, whose stability range is reduced in practice due to actuation saturation.

Since the model-based feedback controllers stabilize the plant over a range of growth rate, it is of interest to investigate the performance of the controllers using a time-varying growth rate  $\gamma$ . The results for a sinusoidal excitation of the  $c_{pp}$  parameter is presented in Fig. 4. The amplitude of the sinusoidal function in  $c_{pp}$  units is  $\pm 5.4175$  with an offset value of 5.75, which results in a function that reaches the highest growth rate in the design range ( $c_{pp} = 0.3325$  or  $\gamma = 5000$ ). Its frequency is 5000 rad/s. Both the LQG and NCF controllers perform satisfactorily and the RWM mode amplitude is quickly suppressed. The PD controller however has difficulty suppressing the RWM amplitude and becomes unstable.

Table 2  
Controller stability ranges.

| Measure           | PD           | LQG          | NCF          |
|-------------------|--------------|--------------|--------------|
| Stability range   | 0–4980 rad/s | 0–9109 rad/s | 0–9027 rad/s |
| Performance range | 0–3278 rad/s | 0–7969 rad/s | 0–8746 rad/s |

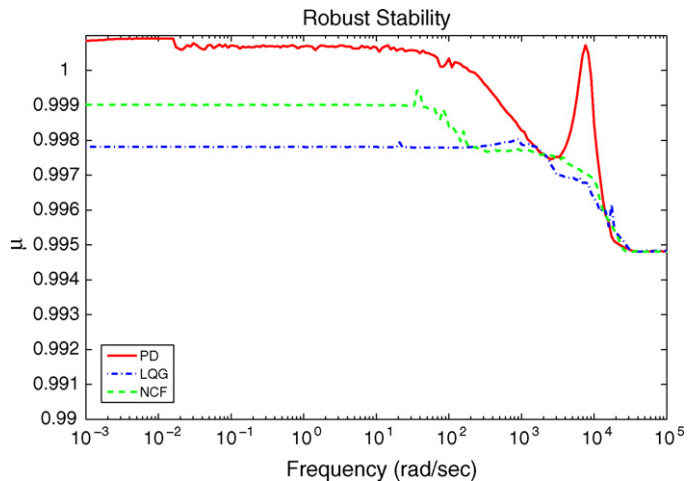


Fig. 5. Robust stability.

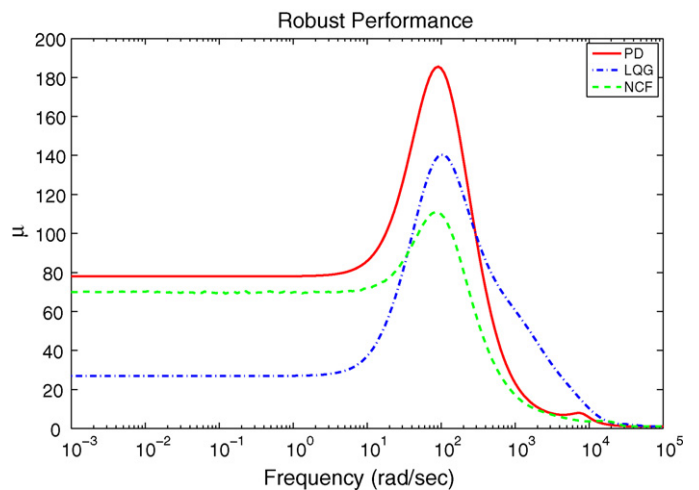


Fig. 6. Robust performance.

#### 5.4. Robust stability and performance metrics

Figs. 5 and 6 show the structured singular values of  $N_{11}$  and  $N$ , respectively as functions of the frequency. The structured singular values were computed using a 29 eigenmode model, with a full range [0.3325,71] of  $c_{pp}$ , centered nominal value, and no reduction of states. The weight function used to define performance (i.e., to shape the frequency response of  $T_{zw}$ ) is of the form  $W_p = (M^{-1/n}s + \omega_b^*)^n / (s + \omega_b^*A^{1/n})^n$ , where  $M = 1$ ,  $\omega_b^* = 10^4$ ,  $A = 10^{-4}$ , and  $n = 2$ . These frequency-domain parameters were selected according to the time-domain specifications given in Table 1. Fig. 5 shows that the PD controller does not satisfy the robust stability condition with a peak value of 1.0009 compared to 0.9982 and 0.9994 for the LQG and NCF controllers. None of the controllers satisfy the performance condition defined by the weight  $W_p$ , but the PD controller achieves the highest peak value of 185.56 compared to 140.43 and 110.95 for the LQG and NCF controllers, which are closer to the satisfaction of the condition. These results are consistent with those presented in Table 2.

## 6. Conclusions

Model-based optimal and robust controllers were successfully synthesized outperforming empirically-tuned non-model-based PD controllers. The performance improvement has been illustrated by time responses, stability and performance ranges, and robust stability and performance metrics. The stability region was improved with the model-based controllers, while maintaining an implementable controller order. Present work includes the implementation of these controllers in DIII-D.

## References

- [1] M.L. Walker, Emerging applications in tokamak plasma control, *IEEE Control Systems Magazine* 26 (2) (2006) 35–63.
- [2] M. Okabayashi, Control of the resistive wall mode with internal coils in the DIII-D tokamak, *Nuclear Fusion* 45 (December) (2005) 1715–1731.
- [3] S. Mauel, Dynamics and control of resistive wall modes with magnetic feedback control coils: experiment and theory, *Nuclear Fusion* 45 (April (4)) (2005) 285–293.
- [4] S. Sabbagh, The resistive wall mode and feedback control physics design in NSTX, *Nuclear Fusion* 44 (April (4)) (2004) 560–570.
- [5] P.R. Brunell, K.E.J. Olofsson, L. Frassinetti, J.R. Drake, Resistive wall mode feedback control in EXTRAP T2R with improved steady-state error and transient response, *Physics of Plasmas* 14 (October (10)) (2007) 1–11, 102505.
- [6] A. Soppelsa, L.M.G. Marchiori, P. Zanca, Design of a new controller of MHD modes in RFX-mod, *Fusion Engineering and Design* 83 (April) (2008) 224–227.
- [7] A. Sen, Optimal control of tokamak resistive wall modes in the presence of noise, *Physics of Plasmas* 10 (November (11)) (2003) 4350.
- [8] O. Katsuro-Hopkins, Enhanced ITER resistive wall mode feedback performance using optimal control techniques, *Physics of Plasmas* 47 (September (9)) (2007) 1157–1165.
- [9] C. Fransson, Model validation, dynamic edge localized mode discrimination, and high confidence resistive wall mode control in DIII-D, *Physics of Plasmas* 10 (10) (2003) 3961–3974.
- [10] Y. In, Model-based dynamic resistive wall mode identification and feedback control in the DIII-D tokamak, *Physics of Plasmas* 13 (2006) 062512.
- [11] D.H. Edgell, Magnetohydrodynamic mode identification from magnetic probe signals via a matched filter method, *The Review of Scientific Instruments* 73 (4) (2002) 1761.
- [12] D.S. Naidu, *Optimal Control Systems*, CRC, 2002, p. 12.
- [13] G.F. Franklin, J.D. Powell, A. Emami-Naeini, *Feedback Control of Dynamic Systems*, Prentice Hall, 2005, pp. 2–3.
- [14] K. Zhou, J.C. Doyle, *Essentials of Robust Control*, Prentice Hall, 1997.
- [15] T. Kailath, *Linear Systems*, Prentice Hall, 1979.
- [16] J. Dalessio, Robust control of resistive wall modes in tokamak plasmas using  $\mu$ -synthesis, in: *Proceedings of the 17th IFAC World Congress on Automatic Control*, 2008.